Research on Water-Vapor Distribution in the Air over Qilian Mountains*

ZHANG Qiang[1†](张 强), ZHANG Jie[1](张 杰), SUN Guowu[1](孙国武), and DI Xiaohong[2](狄潇泓)

1 *Key Laboratory of Arid Climatic Changing and Reducing Disaster of Gansu Province; Key Opening Laboratory of Arid Climatic Change and Disaster Reduction of CMA; Institute of Arid Meteorology, China Meteorological Administration, Lanzhou* 730020

2 *Lanzhou Regional Meteorological Centre, Lanzhou* 730020

(Received November 27, 2007)

ABSTRACT

Based on the remote sensing data, the radiosonde data and precipitation data observed by weather stations, distributions of atmospheric water-vapor and cloud motion wind over the Qilian Mountains are analyzed. Moreover, on the basis of water-vapor and cloud motion wind analyses, relations of atmospheric water-vapor distribution with precipitation, atmospheric circulation, and terrain are investigated. The results show that distributions of atmospheric water-vapor and precipitation in the Qilian Mountains are affected by the westerly belt, the southerly monsoon (the South Asian monsoon and plateau monsoon), and the East Asian monsoon. In the northwest Qilian Mountains, water-vapor and precipitation are entirely affected by the westerly belt, and there is no other direction water-vapor transport except westerly water-vapor flux, hence, the northwest region is regarded as the westerly belt region. In the south and middle of the mountains, water-vapor is mainly controlled by the southerly monsoon, 37.7% of the total water-vapor is from the south, especially in summer, the southerly water-vapor flux accounts for 55.9% of the total, and furthermore the water-vapor content in the southerly flow is more than that in the westerly flow. The southerly monsoon water-vapor is influenced by the South Asian monsoon from the Indian Ocean and the plateau monsoon in the Qinghai-Tibetan Plateau, thus, the south and middle region is called southerly monsoon region. But in the northeast Qilian Mountains, the East Asian monsoon is the main climate system affecting the water-vapor. Besides west and northwest water-vapor fluxes, there are a lot of easterly water-vapor fluxes in summer. The frequency of easterly cloud motion winds in summer half year accounts for 27.1% of the total, though the frequency is not high, it is the main water-vapor source of summer precipitation in this region, therefore, the northwest region is a marginal region of the East Asian monsoon. On the other hand, atmospheric water-vapor, precipitation, and conversion rate of water-vapor into precipitation are closely related with altitudes and circulation system. Generally, there is a peak value of water-vapor content at the altitude from 3500 to 4500 m on the windward slope, but on the leeward slope, water-vapor monotonically decreases with altitude descending except for that in the East Asian monsoon region. Water-vapor on the leeward is much less than that on the windward slope, and the maximal difference in water-vapor content between the two sides may reach about 4.49 kg m^{-2}. Either the values of water-vapor content, precipitation or the conversion rate of water-vapor into precipitation all reach their maxima in the East Asian monsoon regions, and correspondingly the peak value of water-vapor on the windward is also large and occurs at a lower altitude in comparison with other two regions.

Key words: satellite remote sensing data, Qilian Mountains, atmospheric water-vapor, cloud-motion wind, atmospheric circulation

1. Introduction

Qilian Mountains lie in the Central Eurasia, extending from the east of Wushaoling region to the west of Dangjin Mountain, in 37°–40°N, 92°–104°E. Its altitude is between 1700 and 5808 m, and the relative difference of altitude is very large. The mountains border on the Qinghai-Tibetan Plateau on the south and Hexi Corridor on the north. Because of the increasing water domino effect (Ding, 2003), the water-vapor and precipitation are rich in the mountains (Yi et al., 2003). All these factors keep permanent glacier and perpetual snow which feed three inland rivers including Heihe, Shule, and Shiyang Rivers. Therefore,

*Supported jointly by the Ministry of Science and Technology of China under No. 2004BA901A16 and the Natural Science Foundation of Gansu Province under No. 3ZS051-A25-011.

†Corresponding author: zhangq@gsma.gov.cn.

Qilian Mountains play a role of natural reservoir of Hexi Corridor for agriculture, ecology, and human life. However, with economic development, population increasing, and the change of ecological environment, water resources are seriously deficient. The tendency to some extent has destroyed the organic structure of "valley climate-water resources-ecological system", and brought about some negative effects on eco-environment such as valley of inland river shrunk, underground water level decreased, lake dried, and oasis of downriver disappeared (Zhang and Hu, 2002). At present, those eco-environmental questions are focused on the precipitation tendency of upriver of inland rivers, and more concerns are given to develop and utilize the cloud water of Qilian Mountains.

To explore cloud water resources of Qilian Mountains, it is primarily to objectively understand spatial and temporal distribution characters of the water-vapor and the circulation system of atmosphere, because of the notable effects of terrain and circulation systems on the Qilian Mountains (Zhang et al., 2006). The study results have shown that climate in Northwest China is influenced by three circulation systems (Song and Zhang, 2003), i.e., the westerly belt, the South Asian monsoon together with plateau monsoon, and the East Asian monsoon. Qilian Mountains just lie in the confluent region of the three circulation systems (Zhang and Hu, 2002), and are probably influenced by three of them. However, in the mountains, there are only few weather stations such as Qilian, Tuole, and Menyuan Stations, and their altitude differences are large, vertical climate characters are obvious, and precipitation is extraordinarily influenced by circulation system and local environment. Because of those factors, understanding the water-vapor distribution around the mountains is constrained in the previous research.

In this research, water-vapor content and cloud motion wind are retrieved from remote sensing data, and the effect mechanisms of terrain and circulation system on precipitation and water-vapor are also studied. The aim is to offer scientific guidance for exploiting cloud water over the Qilian Mountains and to improve the efficiency of artificial enhancing rain and snow.

2. Data and method

2.1 The region under study

Qilian Mountains are located between Gansu and Qinghai Provinces in Northwest China. Figure 1 shows the mountains, with height contours

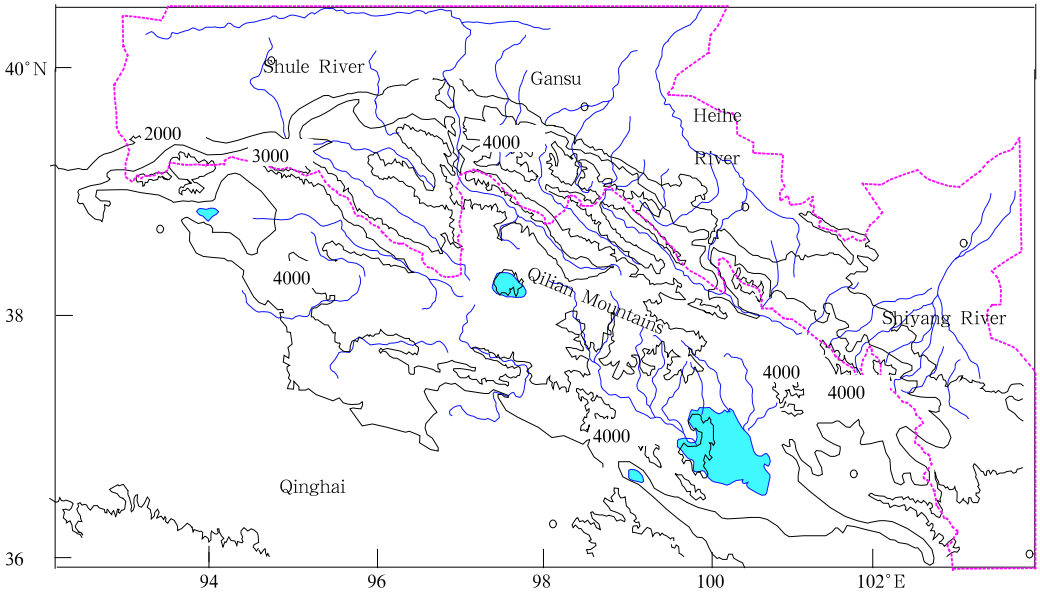

Fig.1. Geographical distribution of the Qilian Mountains. Solid lines are height contours at intervals of 1000 m.

at intervals of 1000 m, and the valley distribution of inland rivers. In Fig.1, Qilian Mountains are wide in range, and terrain trend is from northwest to southeast with many landscapes over the mountains such as grassland, forest, lake, snow cover, and glacier. Because of more than 10 inland rivers such as Heihe, Shule, Shiyang Rivers, and so on, Qilian Mountains form a typical natural environment chain linked by water, and combine precipitation in high mountains with glacier, snow cover, river, oasis, and desert (Hu, 2003). It becomes an eco-environmental union and a landscape of arid region in Northwest China.

2.2 Data

In the research, MODIS data from Terra and Aqua satellites are used, and time series are from May 2002 to April 2005. Meanwhile, hourly GMS data and conventional observed data are also used, including radiosonde data at seven stations around Qilian Mountains from 2002 to 2005 (Li et al., 2005), precipitation of weather stations and hydrological stations from May 2002 to April 2005. The stations are Lanzhou, Dunhuang, Jiuquan, Minqin, Zhangye, Dulan, Xining, Lenghu, and so on. By combining with above data, the water-vapor content and precipitation are analyzed to validate and test retrieval errors.

MODIS sensor onboard Terra and Aqua satellites is one of important components of Earth Observing System. There are 36 narrow bands, the spectrum is between 0.42 and 14.24 μm, and the highest resolution is 250 m. The MODIS has 3 water-vapor absorbed bands and 2 atmospheric window bands, the wavelength centers of water-vapor are 0.905, 0.936, and 0.94 μm, and those of atmospheric window are 0.865 and 1.24 μm. NASA have retrieved water-vapor content <http://modarch.gsfc.nasa.gov/MODARCH> in term of near-infrared specific value algorithm by using the data of 5 bands, and issue the water-vapor content products. The present study uses the 5 bands to retrieve water-vapor content under cloud and cloud-free conditions, but the retrieval errors are large, which is tested by observed data of GPS at Qinghai Stations, therefore, the water-vapor content is retrieved by using optical thickness and efficient radius of cloud particles.

2.3 Calculating method

2.3.1 The method of retrieving water-vapor content by remote sensing

Water-vapor content is the water-vapor mass of unit volume. In meteorology, water-vapor content is defined as the amount of wet air mass of some depth per unit area. At present, there are three methods to retrieve water-vapor content of the atmosphere, i.e., near-infrared method (Kaufman and Gao, 1992; Bennartz and Fscher, 2001), microwave method (Alishouse et al., 1990), and far-infrared method (Ottle et al., 1997; Sobrino et al., 1994). According to the characters of data, the near-infrared method is used in the study to retrieve water-vapor content over the Qilian Mountains.

Under cloud-free conditions, in order to reduce retrieval errors influenced by albedo, one absorbed band and two atmospheric window bands of MODIS are used to retrieve water-vapor content, in which the atmospheric transmittance τ_w is defined as (Gao and Kaufman, 1998)

$$\tau_w = \frac{\rho_{940}}{c_1\rho_{1240} + c_2\rho_{865}}, \tag{1}$$

where ρ_{940}, ρ_{1240}, and ρ_{865} are the reflectance respectively at 940-, 1240-, and 865-nm bands, and c_1(=0.2) and c_2(=0.8) are constants, respectively. When $c_1\rho_{1240} + c_2\rho_{865} \neq \rho_{940}$, we assume $\tau_{1240} = \tau_{865}$ (Wang et al., 2005),

$$\begin{aligned}\tau_w &= \frac{\rho_{940}}{c_1\rho_{1240} + c_2\rho_{865}} \cdot \frac{\tau_{940}}{\tau_{865}} \\ &= \frac{\rho_{940}}{c_1\rho_{1240} + c_2\rho_{865}} \cdot \frac{\rho_{940}}{\rho_{865}} \cdot \exp\left[\alpha + \beta\sqrt{W^*}\right], \end{aligned} \tag{2}$$

$$W^* = mQ_{\rm v} = \frac{1}{\cos\theta} + \frac{1}{\cos\theta_{\rm s}}Q_{\rm v}, \tag{3}$$

where α(=0.02) and β(=0.65) are constants, respectively (Kaufman and Gao, 1992). τ_{1240} and τ_{865} are the transmittance at 1240- and 865-nm bands, θ and $\theta_{\rm s}$ are the zenith angles of sensor and the sun. $Q_{\rm v}$ and W^* are the water-vapor content along the direction of zenith and sensor, then the relation of $\tau_{\rm w}$ and $Q_{\rm v}$ can be obtained.

Under cloud conditions, the information of water-vapor absorption will exist in the ratio value of radiation at two channels because of water-vapor molecules appearing along the route of sun-cloud-sensor, therefore, no matter how thick or thin of cloud optical thickness, aerosols should be considered when water-vapor content is retrieved. Assuming that water-vapor content on the top of cloud is neglected, then, the relation of water-vapor content with cloud optical thickness and cloud effective radius can be formed (Zhang et al., 2006).

Based on the above parameters, the relationship of visibility V, particle size r, and liquid water content $Q_{\rm v}$ may be formulated by definition:

$$V = \frac{C}{Q_{\rm v}} \sum n_r r^3 / \sum n_r r^2 = \frac{C}{Q_{\rm v}} k r_e. \tag{4}$$

As a rule, the optical thickness is taken as that at 550 nm, which is another mode to reflect visibility. According to aerosol and cloud patterns, we have

$$V = \frac{1}{\beta} \ln \frac{1}{\varepsilon} = \frac{3.912}{\beta}, \tag{5}$$

where $\varepsilon(=0.02)$ is the contrast threshold, β is the extinction coefficient of molecule and aerosol at 550 nm, which is correlated to the transmittance τ_w of atmosphere, and the relationship of τ_w and τ can be expressed by

$$\tau_w = \exp(-\tau). \tag{6}$$

According to the attenuation coefficient in the model and Eqs.(4)–(6), the relationship of visibility with optical thickness can be described. In order to directly gain the correlation of visibility with optical thickness τ at 550 nm, a serial of optical thickness values are calculated by using 6S module under the atmospheric module state of middle summer and middle winter, the relationship of visibility V and optical thickness τ is built as follows:

$$V = \frac{4.5254 \times \tau^{-1.0971}}{1000}. \tag{7}$$

Then, the liquid water content of cloud may be expressed by

$$Q_{\rm v} = \frac{2.6 \times r_e}{4525.4 \times \tau^{-1.0971}}. \tag{8}$$

In Eqs.(4)–(8), V is the visibility (m), C is the coefficient (assuming as 2.6 according to scattering theory), and $Q_{\rm v}$ is the liquid water content (g m^{-3}). If there are the same size of all cloud droplets, then k is equal to 1, and k is larger than 1 if the size distribution is in a wide range.

2.3.2 The method of calculating water-vapor by using radiosonde data

According to the definition of water-vapor content, the formula to calculate water-vapor content using radiosonde data can be expressed as below (Liu et al., 2005)

$$Q_{\rm v} = \rho_w \times (H_2 - H_1), \tag{9}$$

where $Q_{\rm v}$ is water-vapor content, ρ_w is water-vapor density, and H_2 and H_1 are the top and bottom heights of water vapor column volume, respectively. The water-vapor content in the research is the total mass content in a column from surface to 100-hPa level, which will be used for testing the retrieval results of MODIS data.

2.3.3 The method of calculating cloud motion wind

Air-flow motion over Qilian Mountains is complicated under the effect of circulation system and terrain. Because of sparse weather stations in Qilian Mountains, it is difficult to understand the motion of air-flow and cloud according to wind property, and cloud characters observed by weather stations. At present, some new researches show that small scale and mesoscale air-flow can be quantitatively estimated by cloud motion wind retrieved from remote sensing data (Xu et al., 1997; Steven et al., 1997).

By statistics of the relative humidity of air at different pressure levels of 7 radiosonde stations in different seasons, the result shows that there are 3 high value levels, i.e., 300, 500, and 700 hPa or near surface. As for Dunhuang, Jiuquan, Zhangye, and Minqin Stations on the north of the mountains, the level of maximum humidity is at 300 hPa except for summer at 500 hPa. The high value of Lenghu Station on the south of the mountains is at 300 hPa except for summer at 400 hPa. As for the east and south of mountains, the level of maximum humidity is at 400–500, and 500 hPa in July. Therefore, on the basis of

the vertical distribution of relative humidity, we can infer that high, middle, and low clouds are situated at about 300, 500, and 700 hPa or near surface.

The research shows that most of precipitation near Qilian Mountains comes from stratus precipitation. In addition, the surface pressure of Qilian Mountains is from 600 to 700 hPa, therefore, when analyzing cloud motion winds, we divide clouds into two types according to whether it can bring on rainfall or not, i.e., high cloud and middle-low cloud. The cloud is considered as high cloud if it is above the level of 400 hPa, and cloud below 400 hPa is considered as middle-low cloud.

Middle-low cloud is researched because it may produce rainfall. Infrared and water-vapor band methods are used for appointing the height of cloud motion wind (Xu et al., 1997), and based on the intercross correlation of infrared and brightness temperature method, the vector of cloud motion wind is evaluated . In the research, the GMS data of 30 min and 1 h are used for analyzing cloud motion wind, the wind vector is expressed by 16 directions, the research region covers 37°–40°N, 92°–104°E, which represents the whole region of Qilian Mountains.

3. Test of retrieval value by using radiosonde observed value

Most of researches show that the water-vapor content calculated from radiosonde data is accurate. In Table 1, observed values of four stations are calculated from radiosonde data. At the same time, the retrieval values of four stations are also done, and the contrast results are given. The table shows that the largest absolute error between retrieval value and observed value is 1.8 kg m^{-2}, most of absolute errors are less than 1 kg m^{-2}, the largest relative error is 14%, and most of relative errors are in ±10%. Because spatial and temporal variation of water-vapor content over Qilian Mountains are remarkable, with a range of more than 10 times, therefore, the above 1 kg m^{-2} errors are tolerable, and the results also show that retrieval values from MODIS can reflect the actual distribution of water-vapor content.

Table 1. Contrast of retrieval value from satellite with observed value of water-vapor content

	Spring				Summer			
	Observed (kg m^{-2})	Retrieval (kg m^{-2})	Absolute error (kg m^{-2})	Relative error (%)	Observed (kg m^{-2})	Retrieval (kg m^{-2})	Absolute error (kg m^{-2})	Relative error (%)
Dunhuang	9.4	8.6	−0.8	−8.5	19.6	20.3	0.7	3.6
Jiuquan	8.8	8.4	−0.4	−4.5	18.2	17.1	−1.1	−6.0
Zhangye	10.1	9.7	−0.4	−4.0	21.6	22.4	1.8	7.4
Minqin	9.3	9.7	−1.3	−14.0	20	20.3	0.3	1.5

4. Results and analyses

4.1 Characters of cloud motion wind and circulation system

In order to discuss the distribution of atmospheric water-vapor content and precipitation, climate characters of air-flow and cloud motion wind are analyzed below, which are important to interpret the effect of circulation system on water-vapor distribution. Here, monthly air-flow and cloud motion wind are analyzed.

Figure 2 depicts sub-area of yearly distribution of cloud motion wind divided by wind vector. Sub-areas show that the direction of cloud motion is mainly controlled by westerly winds, which means that climate is obviously influenced by westerly belts. By analyzing air-flow direction and frequency deviated from westward air-flow, the climate of overall region can be divided into three parts according to air-flow direction.

In sub-area I, the west and northwest of the moun-

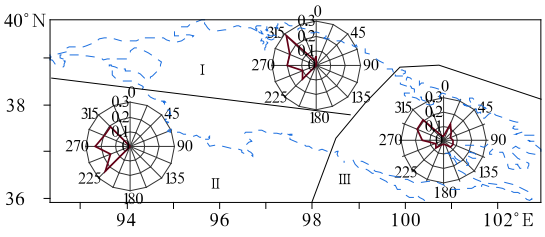

Fig.2. The sub-areas of yearly cloud-motion wind over the Qilian Mountains.

tains, there is no other frequency wind besides west and northwest winds, which means that the region is completely influenced by westerly belts, therefore, it is defined as the westerly belt climate region.

In sub-area II, the middle and south of the mountains, though high frequency wind is from west and northwest, the south wind is also high, whose frequency reaches 37.7%, especially in summer, and wind frequency is more than 55.9%. This air-flow is formed under the effect of South Asian monsoon from the Indian and Plateau monsoon (Huang et al., 2003; Tao and Chen, 1985), which is called the southerly monsoon. Water-vapor content from south is much richer than west and northwest, therefore, the southerly monsoon is more important to the climate of the region, and the region is defined as the southerly monsoon region.

In sub-area III, the east part of the mountains, besides northwest winds, the east wind occurs more remarkable, especially in summer, it reaches 27.1%. Although the east wind is not high, it is influenced by the East Asian monsoon (Huang et al., 2003; Tao and Chen, 1985), and results in a strong precipitation process (Steven et al., 1997), which means that it is more notable summer monsoon of East Asia, therefore, it is defined as the East Asian monsoon region.

Above analysis shows that the Qilian Mountains are a connecting region influenced by westerly belt, southerly monsoon, and the East Asian monsoon. Figure 2 only shows a climate region affected by circulation system in a normal climate year, however, we can infer that the range of each climate region will extend and shrink with monsoon action, and correspondingly a drier year or wetter year appears (Zhang et al., 2006). Therefore, climate in the Qilian Mountains is sensitively and strongly relies on the action of circulation system (Song and Zhang, 2003). Statistical data of 10-yr precipitation show that precipitation anomaly at Tuole Station can reach 65.4%, and its average up to 39.6% in the mountains, which also proved above conclusions.

4.2 Spatial distribution of water-vapor content of atmosphere

Above analyses have shown effects of the circulation system on the Qilian Mountains, different circulation systems will result in different water-vapor distributions. Spatial distribution is drawn by retrieval at 48 grids with 1°×1° resolution. Figure 3 gives water-vapor content distributions, and the tendency of water-vapor content is increasing from northwest to southeast. It is considered that the water-vapor content is high on the east and low on the west, which is decided by the summer monsoon of East Asia. Meanwhile, water-vapor is also high on the south and low on the north, and decided by southerly monsoon. Figure 3 also shows that the gradient tendency from west to east is stronger than that from north to south,

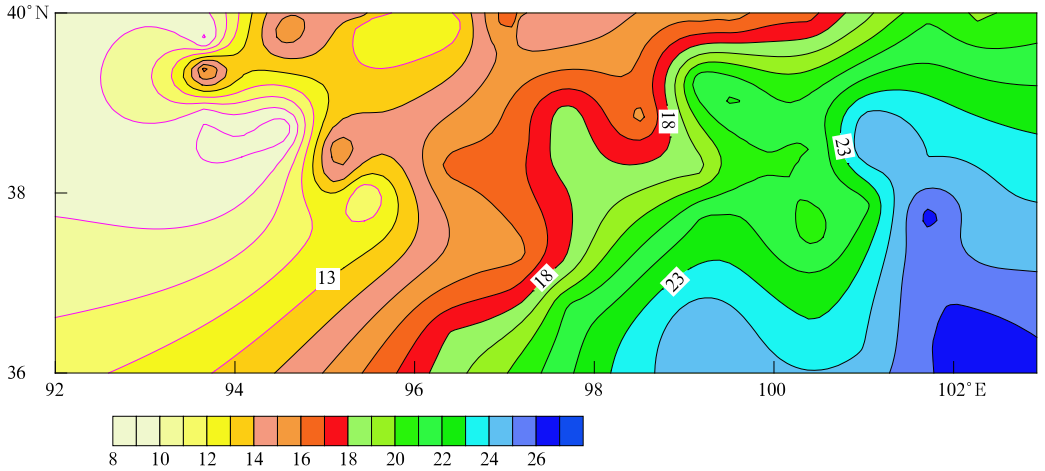

Fig.3. Distributions of annual mean water-vapor content (kg m^{-2}) in the Qilian Mountains and its surroundings.

indicating that the East Asian monsoon and southerly monsoon contribute much water-vapor to the mountains, and the contribution of westerly belt is less than the former two in summer.

At the same time, there are good consistent relations between water-vapor content and terrain, which may be embodied by the disturbance of terrain to water-vapor distribution. Figure 3 shows that the highest and lowest value centers of water-vapor content are related with complex terrain regions, for example, there is a high value center near 38°–39°N, 98°E which is influenced by Shulenan Mountains, and there is a low value center of water-vapor content near 37°–38°N, 100°–101°E on the north of Qinghai Lake. The reason is that there is no altitude difference and the terrain is wide plain.

Meanwhile, it is obvious that the large gradient region of water-vapor content is related with the transitional belt of circulation system, which reflects that it is a typical character of transitional belt of circulation with difference of climate factors.

4.3 Variations of water-vapor content with altitude and slope direction

In order to interpret effects of altitude and slope direction on water-vapor distribution and the relation with circulation system, on the basis of sub-areas from cloud motion wind, the variations of water-vapor content in three regions with altitude and slope direction are given in Fig.4, in which Regions I, II and III represent westerly belt (Fig.4a), southerly monsoon (Fig.4b), and the East Asian monsoon (Fig.4c), respectively, and the relations are also shown in Fig.4. On the windward slope direction, no matter which circulation system affects the region, water-vapor content is well correlated with altitude, and the correlation coefficients of Regions I, II, and III reach 0.931, 0.925, and 0.880, respectively. However, variable characters are different in three regions, the peak values happen at altitude 4608, 3855, and 3476 m, and the peak

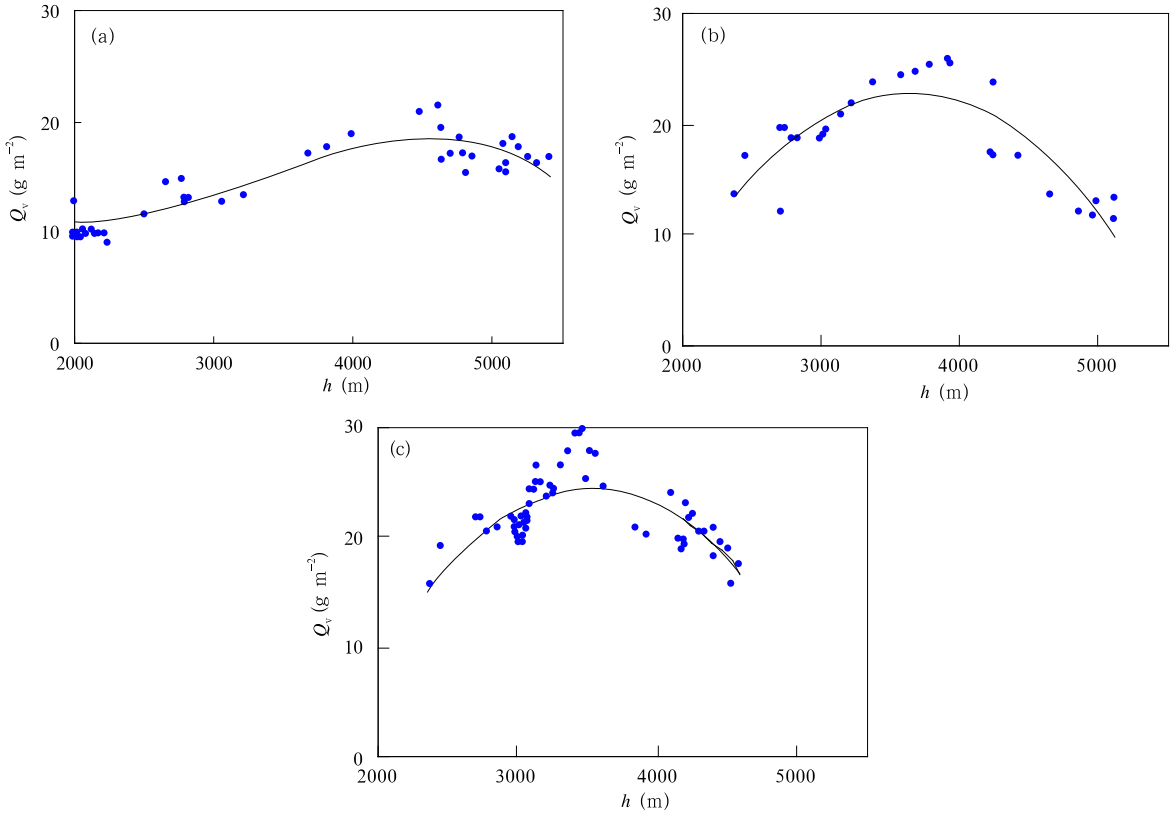

Fig.4. Variations of water-vapor content on the windward slope with height under the circulation system of westerly belt (a), southerly monsoon (b), and the East Asian monsoon (c).

values of water-vapor content are 21.72, 25.75, and 29.58 kg m^{-2}, respectively. The relationships between atmospheric water-vapor content and height in the three regions can be expressed as

$$Q_{v^-(\mathrm{I})} = -2 \times 10^{-7} h^2 + 0.0034h + 5.5922, \quad (10)$$

$$Q_{v^-(\mathrm{II})} = -6 \times 10^{-6} h^2 + 0.0424h - 54.318, \quad (11)$$

$$Q_{v^-(\mathrm{III})} = -7 \times 10^{-6} h^2 + 0.0486h - 61.146, \quad (12)$$

where $Q_{v^-(\mathrm{I,II,III})}$ are atmospheric water-vapor content in three regions (units: kg m^{-2}), and h is height (unit: m).

In comparison of water-vapor contents in the three regions, the water-vapor content in the East Asian monsoon region is the highest, and intensity is the largest, but the altitude of peak value is the lowest. On the contrary, water-vapor contents in Regions I and II are lower, peak values are lower but the altitude of occurrence is higher. The difference of peak value between Regions I and II is about 8 kg m^{-2}, and the altitude difference is more than 1100 m. All those mean that water-vapor content and temperature in Region III are high, so that the cloud forming and development need less terrain forcing. However, in Region I, the water-vapor content of atmosphere is low, and the region is influenced by cold air, therefore, cloud cannot be formed easily, and it needs strong terrain forcing to form cloud. Water-vapor content in Region II is between Regions III and I. It is stirring that the distribution of water-vapor content in this research is consistent with the distribution of precipitation in the previous researches.

Generally speaking, it is different that water-vapor content changes with altitude on the windward and leeward slopes. In order to compare difference, the relationships of water-vapor content with altitude on the leeward slope are given in Fig.5, where Regions I (Fig.5a), II (Fig.5b), and III (Fig.5c) are the same as above. It is obvious that the relationships of water-vapor content with altitude are as well as those on the windward side, and the correlation coefficients in

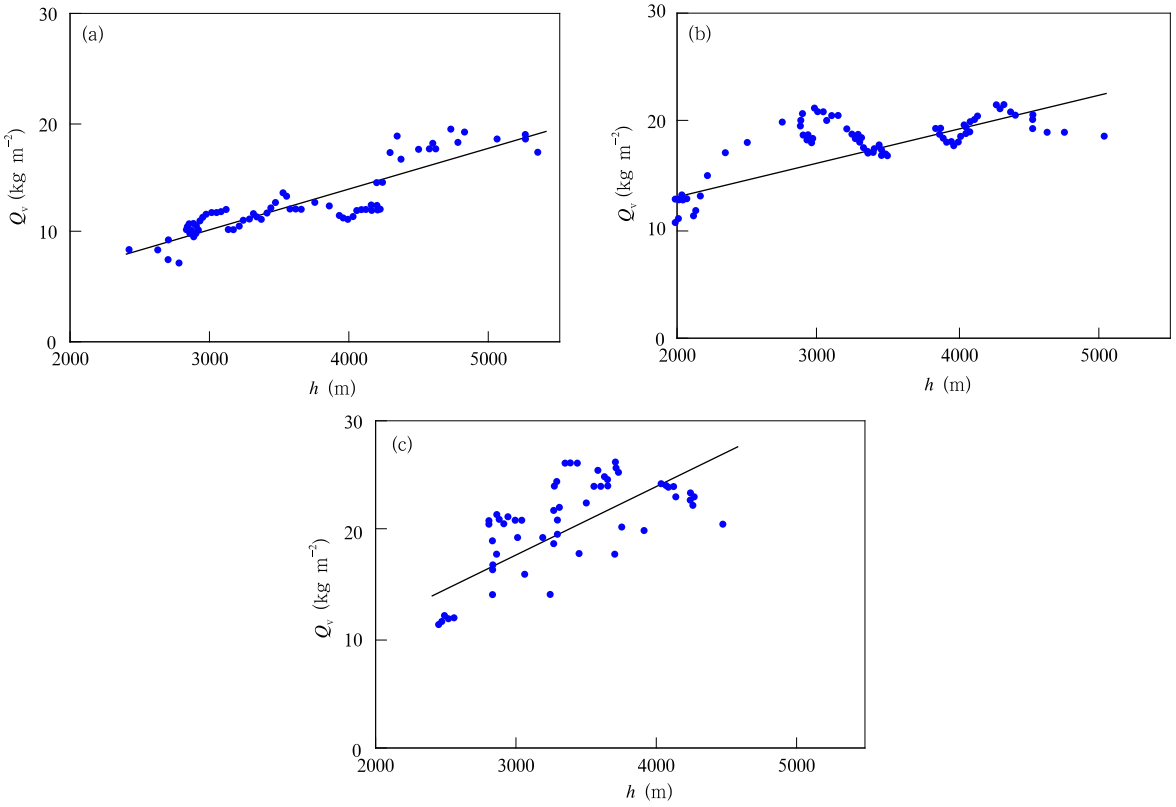

Fig.5. Variations of water-vapor content on the leeward slope with altitude under the circulation system of westerly belt (a), southerly monsoon (b), and the East Asian monsoon (c).

Regions I, II, and III are 0.869, 0.863, and 0.650, respectively.

$$Q_{v^-(\mathrm{I})} = 0.0036h - 0.8668, \tag{13}$$

$$Q_{v^-(\mathrm{II})} = 0.0031h + 6.8532, \tag{14}$$

$$Q_{v^-(\mathrm{III})} = 0.0051h + 3.5661. \tag{15}$$

From Figs.4 and 5, some conclusions can be drawn: Firstly, no matter on the windward or leeward slope, the water-vapor content is increasing with altitude, and there is no peak value generally. Secondly, water-vapor content on the leeward is less than that on the windward, especially in Region I, water-vapor content on the leeward is 0.5–4.49 kg m^{-2} less than that on the windward. Therefore, the vegetation distribution will be different on the two sides of mountains. Above characters may be easily interpreted by the mechanism that when terrain forcing is up to the largest, the precipitation reaches the highest, and water-vapor content gradually decreases with the moving of cloud toward leeward .

4.4 Relationship between water-vapor content and precipitation

Water-vapor content is the basis of precipitation. In order to analyze the relationship of water-vapor with precipitation, three typical regions are taken into account. Figure 6 gives the comparison of precipitation with water-vapor content in Regions I, II, and III. It is obvious that precipitation is well correlated with water-vapor content, and is increasing with water-vapor content, with correlation coefficients 0.973, 0.617, and 0.973, respectively. Compared with the other two regions, the correlation of precipitation with water-vapor content in Region II is lower. One is that precipitation is affected by many complex factors, and the other is that there are no observed data above 4000 m level to contrast. The relationships between precipitation and water-vapor content can be

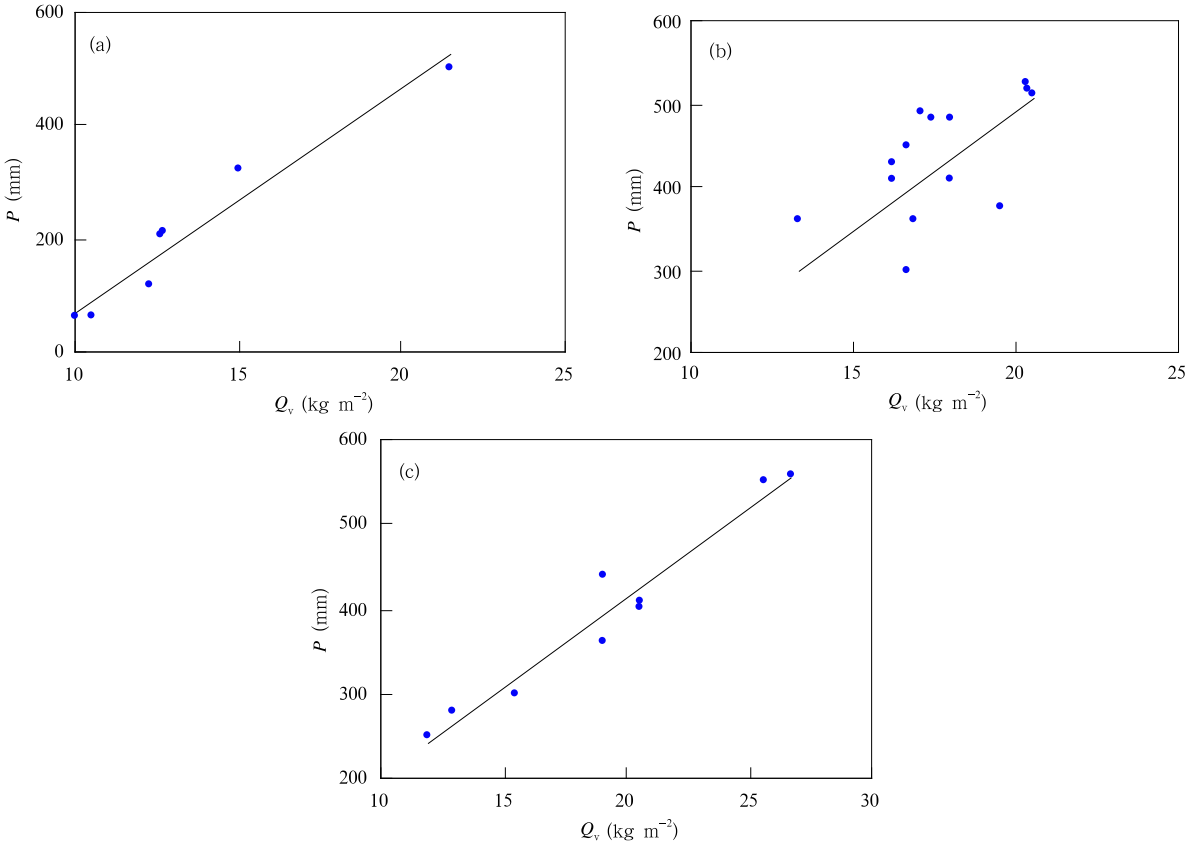

Fig.6. Relationships of annual precipitation with water-vapor content influenced by circulation system of westerly belt (a), southerly monsoon (b), and the East Asian monsoon (c).

expressed as

$$P_{\rm I} = 39.748 \times Q_v - 327.03, \quad (16)$$

$$P_{\rm II} = 28.651 \times Q_v - 82.533, \quad (17)$$

$$P_{\rm III} = 21.193 \times Q_v - 11.664, \quad (18)$$

where variables $P_{\rm I,II,III}$ are the annual average precipitation in Regions I, II, and III (unit: mm).

Figure 7 shows the conversion rate of water-vapor of atmosphere in Regions I, II, and III with altitude. It is obvious that the relation of conversion rate with altitude is very well, and precipitation is increasing with altitude, the correlation coefficient in Regions I and II reach 0.984 and 0.929, respectively, and can be written as

$$f_{\rm I} = -1 \times 10^{-8}h^2 + 0.0001h - 0.079, \quad (19)$$

$$f_{\rm II} = -3 \times 10^{-8}h^2 + 0.0002h - 0.181, \quad (20)$$

where variables $f_{\rm I,II}$ are the conversion rate of water-vapor content to precipitation in Regions I and II P/Q_v(Q_v is transformed from unit kg m^{-2} to mm), unit %. In Region III, the relationship of precipitation with altitude is not obvious, and the conversion rate stabilizes at some degree, meaning that it has reached a high degree in rich precipitation Region III, and it is influenced little by the change of altitude.

By comparing conversion rates with each other in three regions influenced by different circulation systems, it can be seen that the conversion rate of precipitation is different, about 0.175% in Region III, 0.160% in Region II, and 0.145% in Region I, which mean that Region III has the highest conversion rate, Region I has the lowest conversion rate. Above results are more related to precipitation distribution in the east than in the west (Song and Zhang, 2003).

5. Conclusions and discussions

The research shows that it is possible to retrieve water-vapor content by MODIS data, the retrieval value of water-vapor content over Qilian Mountains is consistent with the observed value from radiosonde (Sun, 1981), and can reflect the actual distribution of

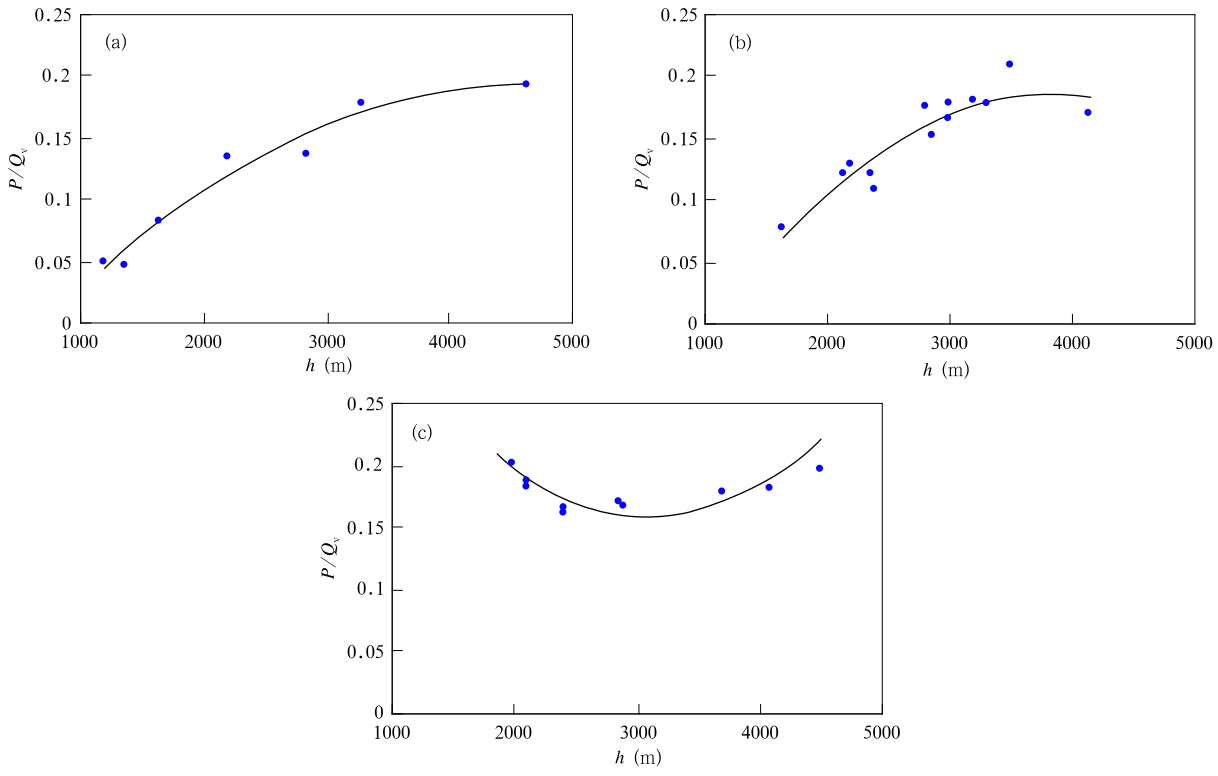

Fig.7. Conversion rates of water-vapor content to precipitation with altitude in Regions I (a), II (b), and III (c).

water-vapor content.

Qilian Mountains are influenced by many climate systems such as westerly belt, southerly monsoon, and the East Asian monsoon. Although the frequency of westerly belt is the highest in the mountains, the richest water-vapor is formed because of the contribution of the East Asian monsoon and southerly monsoon. Moreover, Qilian Mountains are divided into three climate regions, i.e., westerly belt, southerly monsoon, and the East Asian monsoon region, not only by cloud motion wind but also by distributions of water-vapor content, which are proved each other in a physical sense.

In all the three climate regions, the water-vapor content is well correlated with altitudes on the windward slope and leeward slope, but the difference include: Firstly, there is peak value level at 3500–4500 m on the windward slope; secondly, water-vapor content decrease with altitude descending; thirdly, water-vapor contents on the windward slope are more than on the leeward slope, and the most difference is about 4.49 kg m^{-2}, accounting for 30% of the total water-vapor on the leeward slope.

In all the three climate system, the highest water-vapor content is in the East Asian climate region, and the lowest in the westerly belt climate region. Moreover, the water-vapor variation with altitude is different in three climate regions. In the East Asian climate region, water-vapor content is higher on the windward side and the peak-value level is lower. On the contrary, water-vapor content in westerly belt region is lower on the leeward slope, and peak-value level is higher.

Just due to the special effect of circulation system on the distribution of water-vapor content, such precipitation patterns are formed that the precipitation is low in the west while high in the east, and it is low on the plain while high in the mountains. At the same time, the above conclusion is a perfect instruction to the artificial precipitation enhancement region and altitude.

Although many methods and data are used to research the distribution of water-vapor content and influenced mechanism, because of less observation data and low resolution satellite data, it is difficult to test retrieval value and analyze the mechanism deeply. We hope to further study water-vapor question based on the mesoscale monitoring net which will be built in the future.

REFERENCES

Alishouse, J. C., S. A. Snyder, J. Vongsathorn, et al., 1990 : Determination of oceanic total precipitation water from the SSM/I. *IEEE Transactions on Geosciences and Remote Sensing*, **28**, 811–816.

Bennartz, R., and J. Fscher, 2001: Retrieval of columnar water vapor over land from backscattered solar radiation using the Medium Resolution Imaging Spectrometer. *Remote Sensing of Environment*, **78**, 274–283.

Ding Xianrong, 2003: Water increasing effect of mountains and its value of water resources. *Journal of Mountain Science*, **21**(6), 681–685. (in Chinese)

Gao B. C., and Y. J. Kaufman, 1998: Algorithm Technical Background Document: The MODIS Near-IR Water Vapor Algorithm. <http://www.gsfc.NASA.gov/MODIS-Atmosphere/-docs/atbd-mod03>.

Hu Yinqiao and Zuo Hongchao, 2003: Forming mechanism of oasis environment and building countermeasure of ecological environment in arid area. *Plateau Meteorology*, **22**(6), 537–544. (in Chinese)

Huang Ronghui, Chen Wen, and Ding Yihui, 2003: Studies on the monsoon dynamics and the interaction between monsoon and ENSO cycle. *Chinese Journal of Atmospheric Sciences,* **37**(4), 484–498. (in Chinese)

Kaufman, Y. J., and Gao B. C., 1992: Remote sensing of water vapor in the near IR from EOS/MODIS. *IEEE Transactions on Geosciences and Remote Sensing*, **30**(5), 871–884.

Li Guochang, Chen Qian, Chen Tianyu, et al., 2005: Climate character of terrain precipitation in Qilian mountains. *Advances in Earth Science*, **20**, 167–176. (in Chinese)

Liu Shixiang, Yang Jiancai, Chen Xuejun, et al., 2005: The temporal-spatial distribution of vapor content and vapor transportation of Gansu Province. *Meteorological Monthly*, **31**(1), 50–54. (in Chinese)

Ottle, C., S. Outalha, C. Francois, et al., 1997: Estimation of total atmospheric water vapor content from

split-window radiance measurements. *Remote Sensing of Environment*, **61**, 410–418.

Sobrino, J. A., Z. L. Li, M. P. Stoll, et al., 1994: Improvement in the split window technique for land surface temperature determination. *IEEE Transactions on Geosciences and Remote Sensing*, **32**, 243–253.

Song Lianchun and Zhang Congjie, 2003: Variable character of precipitation in Northwest China in recent 20 century. *Journal of Glaciology and Geo-cryology*, **25**(2), 143–148. (in Chinese)

Steven, J., W. Paul, Christopher, et al., 1997 : Fully automated cloud drift winds in NESDIS operations. *Bull. Amer. Meteor. Soc.*, **28**(6), 1234–1245.

Sun Guowu et al., 1981: A study of the lows at 500-mb level over the Qinghai-Xizang plateau in summer. *Geological and Ecological Studies of Qinghai-Xizang Plateau*. New York: Gorton Land Breach, Science Publishers. INC. 1547–1551.

Tao Shiyan and Chen Longxun, 1985: The East Asian summer monsoon. Proceedings of International Conference on Monsoon in the Far East. Tokyo, 1–11.

Wang Weimin, Sun Xiaomin, Zhang Renhua, et al., 2005: The simulation analyses of the effect of surface reflective spectrum on the retrieval of water vapor with MODIS Nir data. *Journal of Remote Sensing*, **9**(1), 8–15. (in Chinese)

Xu Jianmin, Zhang Qisong, and Fang Xiang, 1997: Height assignment of cloud motion winds with infrared and water vapour channels. *Acta Meteor. Sinica*, **55**(4), 408–416. (in Chinese)

Yi Shuhua, Liu Hong, and Li Weiliang, 2003: Spatial and temporal distributions of cloud over Northwest China. *Meteorological Monthly*, **29**(1), 7–11. (in Chinese)

Zhang Jie, Zhang Qiang, and He Jinmei, 2006: Remote sensing retrieval and analysis of optical character of cloud in Qilian Mountains. *Acta Meteor. Sinica*, **20**(suppl.), 69–75. (in Chinese)

Zhang Qiang and Hu Yinqiao, 2002: Geological character of oasis and climate domino effect. *Advances in Earth Science*, **17**(4), 477–486. (in Chinese)